



# Simultaneous prediction of steam production and reduction efficiency in recovery boilers of pulping process



Arthur Damasceno, Lucas Carneiro, Nayana Andrade, Suênia Vasconcelos, Romildo Brito, Karoline Brito\*

Federal University of Campina Grande, Department of Chemical Engineering, Campina Grande, PB, 58109-970, Brazil

## ARTICLE INFO

### Article history:

Received 27 February 2020

Received in revised form

24 August 2020

Accepted 3 September 2020

Available online 13 September 2020

Handling editor: Cecilia Maria Villas Bôas de Almeida

### Keywords:

Pulp and paper

Pulping (kraft) process

Modeling

Simulation

Aspen plus.

## ABSTRACT

The role of the recovery boiler in the process of pulping is vital as it renders the industrial plant environmentally and economically viable. This boiler reduces the environmental impact of directly disposing liquor. Moreover, the equipment produces “green” steam without the use of fossil fuels as it burns the byproduct (black liquor). The reduction efficiency is the most important variable used to verify the completeness of black liquor combustion. However, because of the need to ensure green steam production, vapor generation in recovery boilers has become an important variable for evaluation. In the literature, only one of the cited variables (reduction efficiency and vapor generation) is found at a time. In this study, a recovery boiler is simulated using Aspen Plus® commercial software to determine the effect of airflows on both the reduction efficiency and green steam production simultaneously. The free energy minimization method is used to predict the composition and production of smelt and the composition of exhaust gas. The results are compared with industrial and literature data, and the model predictions are found to agree with the measurements. Furthermore, a sensitivity analysis is performed on the airflow rates to verify the possibility of increasing steam production without impairing the reduction efficiency. The observations indicated a feasibility of increasing steam by 1 t/h, resulting in a reduction of 675,840 Nm<sup>3</sup>/year of natural gas usage in conventional boilers. Reduction of CO, SO<sub>x</sub>, and NO<sub>x</sub> emissions by 57, 76, and 22%, respectively, can also be achieved owing to these improved airflow rates.

© 2020 Elsevier Ltd. All rights reserved.

## 1. Introduction

### 1.1. Background

The annual global consumption of paper is approximately 500 million tonne, which represents an average of 58 kg per citizen (Munoz et al., 2020). Population increase and the improved social status of individuals have contributed to the high demand for paper (Bhardwaj et al., 2018). Consequently, the paper manufacturing industry is a vital contributor to sectors ranging from packing to storage. Increased industrial activity and growing population have led to a scarcity of natural resources. Owing to community pressure towards conservation of resources, leaders have adopted a tougher stance on implementing sustainable and environment friendly practices (Azevedo et al., 2020; Mardoyan and Braun, 2015).

Therefore, industries are faced with the challenge of balancing profitable practices and adhering to environment friendly regulations. Stricter regulations will result in an increased number of companies disclosing their environmental and social performance (Vochozka et al., 2016).

The method by which pulp for paper manufacture is obtained involves the extraction of cellulose from wood by the removal of lignin and inorganic compounds. This can be achieved in two methods, i.e., by adding either sulfite or sulfate. The most widely used pulping method, known as kraft process, uses sulfate to produce high-performance cellulose (Blasio et al., 2019), as depicted in Fig. 1.

In this process, wood is first chopped into chips and then sent to a digester, where they are cooked at a high temperature and pressure with concentrated white liquor (solution of NaOH and Na<sub>2</sub>S). The role of digester is to remove lignin from wood chips. Its output contains unbleached pulp and weak black liquor.

The remaining lignin imparts a dark color to the unbleached pulp. This is removed using the two-step delignification process

\* Corresponding author.

E-mail address: [karoline.dantas@ufcg.edu.br](mailto:karoline.dantas@ufcg.edu.br) (K. Brito).

Nomenclature			
$\alpha_i$	Weighting coefficient in black liquor decomposition	$H_2O^{OUT}$	Percentage of water in dry black liquor [%]
BL	Black liquor	HHV	High heating value [MJ. Kg <sup>-1</sup> ]
CFD	Computational fluid dynamics	LHV	Lower heating value [KJ. Nm <sup>-3</sup> ]
$C_{Fix}$	Fixed carbon	NG	Natural gas
Conv	Drying efficiency [%]	PR-BM	Peng-Robinson Boston-Mathias
DGSFRM	Solid standard Gibbs free energy of formation [KJ.mol <sup>-1</sup> ]	PROX	Proximate analysis
DHLSUSR	Molar enthalpy of fusion [KJ.mol <sup>-1</sup> ]	Q	Energy stream [cal. s <sup>-1</sup> ]
DHSFRM	Solid standard enthalpy of formation [KJ.mol <sup>-1</sup> ]	RE	Reduction efficiency [%]
$f_{steam}$	Steam flow rate [t/h]	TRS	Total reduced sulfur
$f_{primary}^{air}$	Primary air flow rate [Nm <sup>3</sup> . h <sup>-1</sup> ]	$T_{feedwater}$	Boiler feedwater temperature [°C]
$f_{secondary}^{air}$	Secondary air flow rate [Nm <sup>3</sup> . h <sup>-1</sup> ]	$T_{vap}$	High pressure steam temperature [°C]
$H_2O^{IN}$	Percentage of water in wet black liquor [%]	ULT	Ultimate analysis
		Wet-BL	Wet black liquor
		$X_i$	Mass fraction of component i [%]

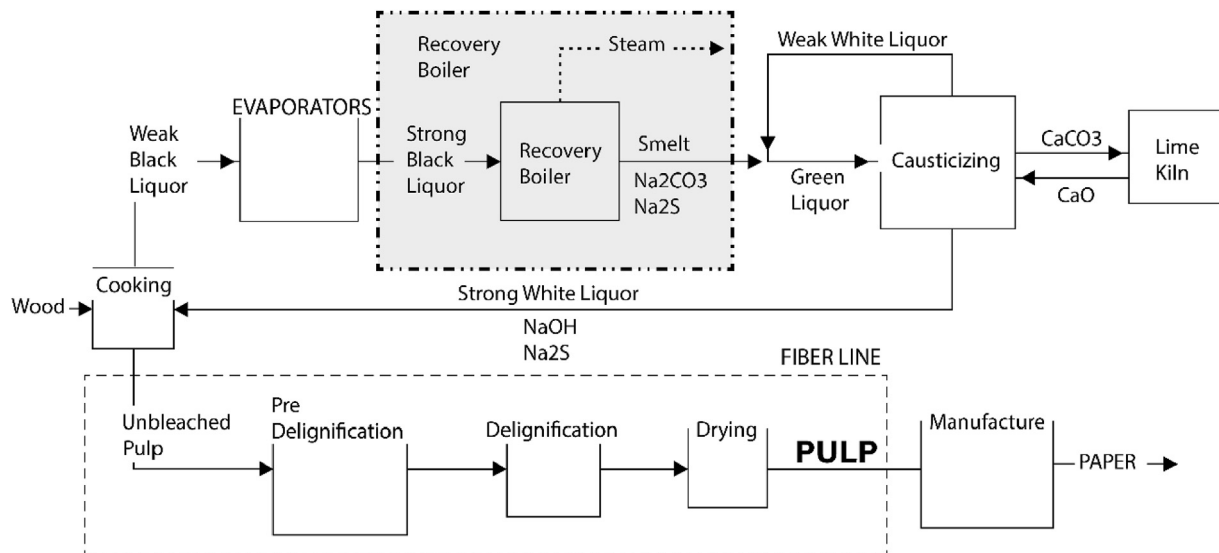


Fig. 1. Simplified block flow diagram of kraft process.

(technology of extracting lignin) that follows, and the resultant bright pulp goes through a drying process to eliminate the residual water. Finally, the dried pulp is sent to a paper-making machine.

The byproduct of this process is weak black liquor, composed of water, the major component, and lignin and inorganic sodium salts. This liquor must be concentrated (through evaporators) to the maximum solid content such that the resulting strong black liquor can be burned in the recovery boiler. Steam is generated in the boiler and all inorganic compounds are recovered in smelt form (a molten salt mixture, mainly comprising  $Na_2CO_3$  and  $Na_2S$ ). The efficiency at which the recovery boiler recovers the chemicals is a direct indication of its performance, known as reduction efficiency. This study focuses on the recovery boiler (as highlighted in Fig. 1) in the context of its reduction efficiency and steam production.

Green liquor, obtained by mixing molten smelt with a diluted (weak) white liquor, is used to recover white liquor in a causticizing section. In this process, green liquor reacts with  $CaO$  (quick lime), producing white liquor and  $CaCO_3$  (lime mud). The white liquor is recycled back to the beginning of the process. The lime mud obtained is calcined in a lime kiln, where quick lime is generated and recycled back to the causticizing process (Hu et al., 2020).

According to Azevedo et al. (2020), the high volume of solid waste generation is a major drawback of the pulp and paper industry. Black liquor is the main byproduct of paper and pulp processing. However, black liquor retains over half of the energy contained in the wood fed into the digester. Hence, black liquor has been used as an additional energy source since 1930 (Blasio et al., 2019). Burning the organic compounds in the black liquor generates energy in the form of high-pressure steam (Ferreira et al., 2010), which is used to produce electricity. It is estimated that the amount of energy produced by burning black liquor exceeded 71.4 billion kWh in 2017 (EIA, 2017).

It is noteworthy that the energy requirement in the pulp and paper industry is fulfilled by both recovery and classical boilers. In a conventional boiler, natural gas is typically used as fuel. Meanwhile, the recovery boiler uses a byproduct (black liquor). If the performance of the recovery boiler is improved, more steam can be produced. Therefore, the requirement of natural gas in classical boilers can be reduced. Furthermore, the recovery boiler should recover the highest content of inorganic compounds.

Two parameters are important for evaluating the recovery boiler: inorganic compound recovery and steam generation. To

consider the two parameters simultaneously, the entire process should be modeled. However, complications in recovery boilers occur owing to the high diversity of physical and chemical transformations during the black liquor burning, which increases the difficulty of mathematical modeling. Hence, only part of the equipment has been modeled in previous studies. This strategy is not always efficient as the equipment is highly integrated; the performance of one section affects that of the other. Therefore, it is beneficial to develop a complete model that includes the main parameters. Developing new strategies to deal with unsolved problems improve process performance while result in a more competitive business (Ungerman et al., 2018).

### 1.2. Previous studies

The modeling of recovery boiler is typically performed through computational fluid dynamics (CFD). The Institute of Paper Chemistry published the first paper using CFD techniques to simulate a recovery boiler, employing Fluent software for numerical calculations (Jones, 1989). Since then, many papers have been published regarding this topic, in which numerical algorithm improvements have been employed. Hence, deeper understanding of mathematical modeling, development of new procedures to optimize operation conditions, and improvements in the geometry of recovery boilers have been achieved, thereby affording an efficient and stable operation of the equipment.

Using CFD is important for evaluating a process in the microscopic scale. Maakala et al. (2018) modeled a superheater using CFD and validated it with experimental data. Leppänen et al. (2014) used CFD to simulate fine fume particles resulting from the condensation of alkali compound vapors in a recovery boiler. Pérez et al. (2016a) developed a CFD model that can predict ash deposition and scale growth in recovery boilers. The authors also published a study, based on the Lagrangian method, presenting the dynamic state CFD analysis of ash deposition (Pérez et al., 2016b). Recently, Pérez et al. (2019) compared 2D and 3D mesh models. However, CFD techniques are computationally expensive and time-consuming.

Artificial intelligence can be used to model recovery boilers because a large amount of data is available in industry, as shown by Sainlez et al. (2011), who predicted the rate of vapor flow in a recovery boiler using artificial neural networks. Artificial neural networks, however, require a large amount of data to learn correct tasks and calculate well, compared to data outside of the training set (Machová and Vochozka, 2019). Additionally, evaluation of equipment performance becomes difficult when a novel input is outside the range of training data.

The macroscopic approach enables the operating conditions of a process to be optimized. Using the Visual C++ environment, Ghaffari et al. (2003) simulated the steady state of the lower part of a boiler. Cardoso et al. (2012) simulated the combustion stage of a boiler using the WinGEMS commercial software. The authors aimed to evaluate the effect of increasing the dry solid content of a black liquor on the boiler. Silva et al. (2008) used Gibbs free energy minimization to determine the composition of a smelt. However, they did not evaluate the effects of different air flow rates on smelt formation and steam generation.

Other researchers have been using Aspen Plus® to represent a single equipment that plays complicated operations to consider modeling with a macroscopic point of view. Taking advantage of the Aspen Plus® library, the complete equipment is split into small units, each representing a zone where a specific phenomenon occurs. This approach allows the user to build a variety of models, even when the equipment is not present in the software. Qin and Chang (2017) simulated a coke oven used to produce coke from

coal, Zhang et al. (2011) represented a rotatory kiln, and Han et al. (2017) developed a model of downdraft biomass gasification.

The inorganic compound recovery and steam generation are the most important responses in a recovery boiler. The inorganic compound recovery is evaluated in the lower section, while the steam generation is analyzed in the upper section of the equipment. Thus, the simultaneous evaluation of both parameters is possible.

The hypothesis of this work is that simultaneous evaluation of the main parameters is possible by splitting the complete recovery boiler into small sections, each one representing a main phenomenon. To the best of our knowledge, there are no published studies that have simulated all sections of a recovery boiler in a unique model.

### 1.3. Aim and novel contribution

Previous studies typically encompass only a part of the problem; some studies focused on smelt formation, whereas others focused on steam generation. However, both smelt and steam are critical products in recovery boilers, and the production of one may impacts that of the other.

In this study, it was developed a rigorous model of a recovery boiler using Aspen Plus®. All the regions of the equipment were considered. Thus, the chemical composition of the smelt at the bottom of the boiler and the green steam generation in the upper section could be calculated at once. We regarded this model as a useful tool for understanding and evaluating the recovery boiler macroscopically as the most important variables were considered.

The developed model enables the evaluation of other operational conditions. Through sensitivity analysis, a scenario can be observed wherein green steam can be increased, the emission of polluting gases is reduced, and the required inorganic recovery is maintained. This improvement in recovery boilers diminishes the need for natural gas-based conventional boilers and, thus, also has an environmental impact owing to cleaner exhaust gas emissions.

Hence, the developed model in this study is more eco-efficient, implying that the natural resources required in the processes are used more efficiently (Yu et al., 2015, 2016). In fact, an eco-efficient production will help improve the competitiveness of industries because it enables wider profit margins.

Finally, the model was validated with data from the literature and from the largest pulp and paper mill in Latin America. Real data from this process are difficult to obtain in the literature, rendering the data presented herein highly valuable. It is important to highlight that coalescence of industry and academy results in successful technological innovations, which are essential for creating and sustaining an organization's competitive advantage (Hana, 2013).

## 2. Process description

Recovery boilers currently in use remain largely unchanged from its original evolution based on the work of Tomlinson (1969).

The recovery boiler comprises two regions: a lower region (furnace) where smelt is formed, and an upper region (superheaters, boiler bank, and economizer) for generating superheated steam. The “nose” separates these two sections. The process of burning black liquor begins when the black liquor is fed into the lower region through spray nozzles located on the furnace walls (Silva et al., 2008). According to Grace (1992) and Smook (1989), burning black liquor involves several steps, with each step occurring in a different section of the boiler, as shown in Fig. 2.

The boiler typically involves an injection of primary, secondary, and tertiary air (modern boilers have quaternary air as well). The air injection configuration significantly affects the reduction efficiency

and steam production. Each injection has a different function in the complex chemical process that occurs inside the equipment.

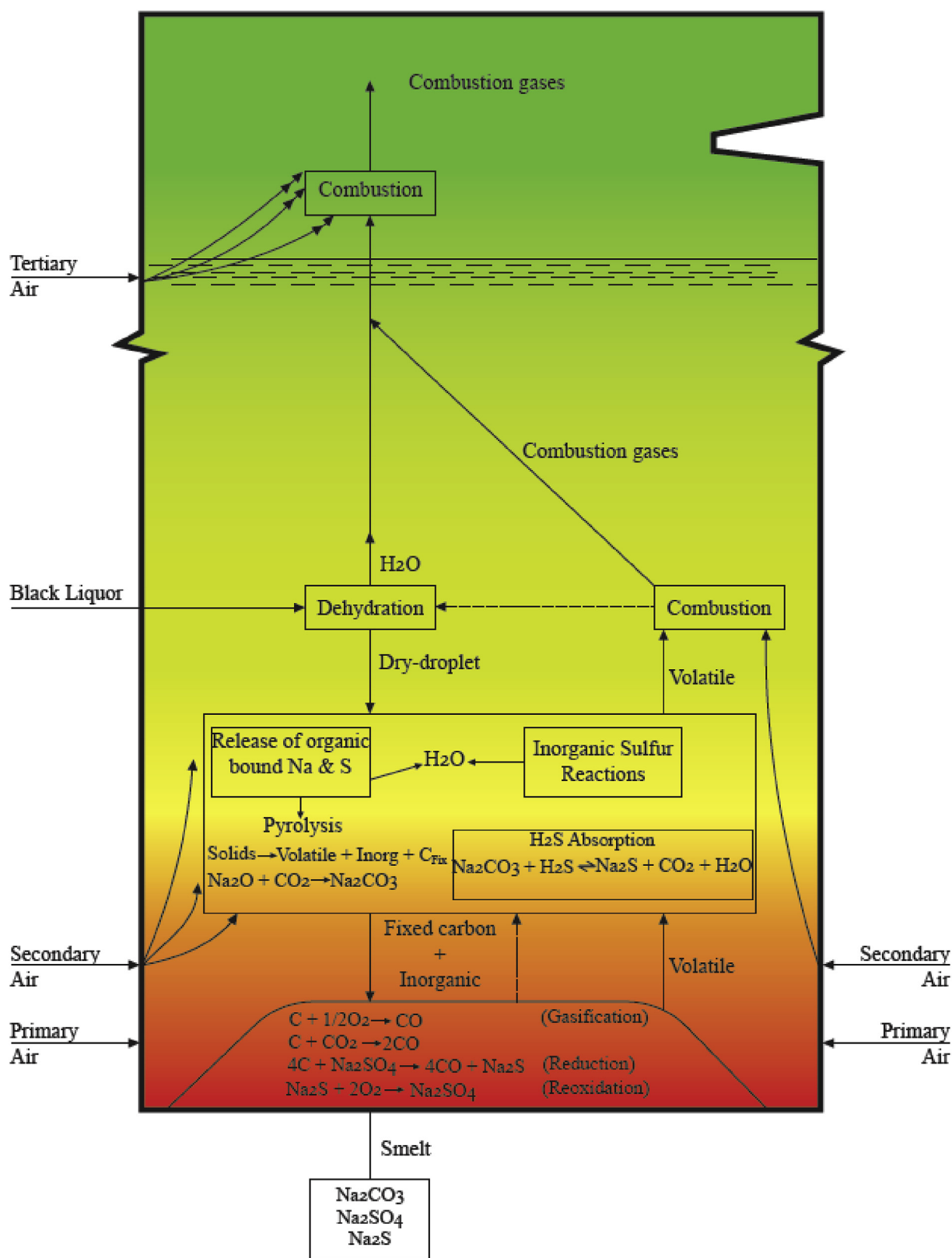


Fig. 2. Main reactions in a recovery boiler of the pulping process.

In the drying stage, black liquor is exposed to flue gases from the bottom of the boiler and loses its residual moisture. The black liquor then degrades to form a mixture of total reduced sulfur (TRS) volatiles ( $\text{CH}_3\text{SH}$ ,  $\text{CH}_3\text{SCH}_3$ ,  $\text{CH}_3\text{S}_2\text{CH}_3$ ,  $\text{H}_2\text{S}$ ),  $\text{SO}_2$ ,  $\text{CO}_2$ ,  $\text{CO}$ ,  $\text{CH}_4$ ,  $\text{H}_2\text{O}$ , and a porous particulate material. This stage corresponds to pyrolysis and comprises irreversible chemical reactions.

In the region above the pyrolysis section, the gases react with the  $\text{O}_2$  of the secondary and tertiary air to provide energy for green steam generation. In addition, the tertiary air ensures that polluting gases, such as  $\text{CO}$  and TRS, do not permeate beyond this section. Meanwhile,  $\text{H}_2\text{O}$  and  $\text{CO}_2$  flow to the upper region of the boiler, leaving exhaust gases in the equipment.

The porous particulate material is composed of inorganic salts, primarily  $\text{Na}_2\text{SO}_4$ ,  $\text{Na}_2\text{S}$ ,  $\text{Na}_2\text{CO}_3$ , and fixed carbon. The combustion of the fixed carbon with the  $\text{O}_2$  from the primary air provides energy for the endothermic reaction of  $\text{Na}_2\text{SO}_4$  that will occur in the char bed, in particular, the reaction of carbon with  $\text{Na}_2\text{SO}_4$  to form  $\text{Na}_2\text{S}$ . The lower region of the recovery boiler must have a reducing environment with no  $\text{O}_2$  to prevent a reaction between  $\text{Na}_2\text{S}$  and  $\text{O}_2$  in the primary air to form  $\text{Na}_2\text{SO}_4$ . The occurrence of this reaction will reduce the reduction efficiency of the boiler.  $\text{Na}_2\text{S}$  and  $\text{Na}_2\text{CO}_3$  form smelt, a molten salt mixture.

Furthermore, each region of the boiler comprises a complex set of exothermic and endothermic chemical reactions that require specific operating conditions to ensure the stable operation of the process.

### 3. Process modeling

The recovery boiler modeling was performed using Aspen Plus®. This process-simulation program provides an estimate of the parameters of a process (pressure, temperature, and composition) under specific conditions by solving mass and energy balance relations within the limitations of a phase equilibrium database. In addition, this software can manage unconventional materials, such as coal or black liquor.

For modeling, the recovery boiler was conceptually divided into subunits, with adjacent subunits interconnected by energy and material balance, as described later. The developed model includes the lower (reactive zone) and upper (steam generation) regions of the equipment.

#### 3.1. Assumptions

The following assumptions were considered in modeling the recovery boiler:

- ✓ The model is zero dimensional: the output variables were evaluated in relation to the input variables without considering the details of the processes occurring inside the control volume;
- ✓ The assumption above typically requires chemical and thermodynamic equilibria to be considered;
- ✓ The process is steady state;
- ✓ The char bed contains only  $\text{Na}_2\text{SO}_4$ ,  $\text{Na}_2\text{CO}_3$ , and  $\text{Na}_2\text{S}$ ;
- ✓ The ash is inert;
- ✓ The recovery boiler operates at 1 bar.

The considerations above were based on literature review and did not markedly affect the validity of the simulation results.

#### 3.2. Thermodynamic model

The Peng Robinson–Boston Mathias (PR–BM) equation of state was selected as the global property method to calculate the properties of different components during the entire process. This

thermodynamic model uses the Peng–Robinson cubic equation of state with the Boston–Mathias alpha function for all the thermodynamic properties, which is suitable for hydrocarbons and light gases (Aspentech, 2001). This model requires the same set of equations to be solved for both liquid and vapor phases. The PR–BM method is typically applied to biomass gasification and pyrolysis processes (Gagliano et al., 2017; Shahbaz et al., 2017; Lide, 2003).

Black liquor is modeled as an unconventional solid; therefore, properties for characterizing this solid must be calculated. These properties are enthalpy and density, calculated using the HCOALGEN and DCOALIGT models, respectively, in which proximate and ultimate analyses are required. The HCOALGEN and DCOALIGT property models include different correlations to calculate the heat of combustion, heat of formation, and heat capacity of the solid. As the heat of combustion was known, its value was used in the model.

Values of the enthalpies (DHSFRM) and free energies (DGLSFRM) of formation and the enthalpy of fusion (DHLSUSR) of  $\text{Na}_2\text{CO}_3$ ,  $\text{Na}_2\text{O}$ ,  $\text{Na}_2\text{S}$ , and  $\text{Na}_2\text{SO}_4$  were not available in the simulator library. Hence, these data were obtained from Lide (2003), as shown in Table 1.

#### 3.3. Input data

Prior to entry into the boiler, the black liquor must be concentrated to increase its energy efficiency during combustion. Accordingly, the weak black liquor must be concentrated until the dry solids reached 70% of the total composition, the remaining 30% being moisture. It was assumed that the black liquor was initially at 130 °C. The ultimate analysis, shown in Table 2, was obtained from the largest pulp and paper manufacturer in Latin America. The average operating conditions were obtained directly from the industrial dataset (Table 3).

#### 3.4. Aspen Plus® model

The recovery boiler can be regarded as a chemical reactor, as inorganic compounds are recovered as smelt (Silva et al., 2008). A kinetic free equilibrium steady-state model has been developed. Owing to the complexity of black liquor combustion in recovery boilers, only the major steps of this process were considered in the

**Table 1**  
Information of missing parameters.

	$\text{Na}_2\text{CO}_3$	$\text{Na}_2\text{O}$	$\text{Na}_2\text{S}$	$\text{Na}_2\text{SO}_4$
DHSFRM (kJ/mol)	−1131.0	−416.0	−370.3	−1384.6
DGSFRM (kJ/mol)	−1047.5	−377.1	−354.8	−1266.8
DHLSUSR (kJ/mol)	28.0	—	6.7	24.3

**Table 2**  
Ultimate analysis of black liquor (dry basis).

Component (wt%)	C	H	Na	S	Cl	O	$\text{Na}_2\text{CO}_3$	$\text{Na}_2\text{SO}_4$
	34.53	3.4	14.25	2.73	1.54	28.08	9.44	6.03

**Table 3**  
Normal conditions of operation.

Variables	Value
Black liquor flow rate (kg/s)	22.37
Solids content (%)	70.00
High heat value, HHV (MJ/kg)	13.34
Primary air ( $\text{Nm}^3/\text{h}$ )	45,460
Secondary air ( $\text{Nm}^3/\text{h}$ )	88,960
Tertiary air ( $\text{Nm}^3/\text{h}$ )	44,163



model. When the black liquor particles traveled through a recovery boiler, drying, pyrolysis, combustion, and reduction reactions occurred. Costa et al. (2004) reported that the chemical reactions occurred simultaneously in the solid phase. The ultimate chemical species melted to form the smelt only after chemical equilibrium has been attained. Hence, the Gibbs free energy minimization method was employed to determine the distribution and composition of the multiphase mixture in the recovery boiler.

As Gibbs free energy minimization is a nonstoichiometric method, it can overcome the fact that the black liquor has no defined chemical formula. This method is represented by the RGibbs block. This module uses an algorithm based on the studies of Gautam and Seider (1979) and White and Seider (1981).

Each section was implemented in a hierarchy block, as shown in Fig. 3. Mass and energy flows were coupled to represent the overall process. The details of each section are provided in the following subsections.

Table 4 is a summary of the routines representing the chemical recovery boiler, with the description and purpose of each briefly outlined.

#### 3.4.1. Drying section

Fig. 4 shows the drying region. The black liquor (WET-BL) feeds the boiler, and gases from the lower sections (VOLAT-2) remove the remaining moisture from the black liquor droplets through evaporation.

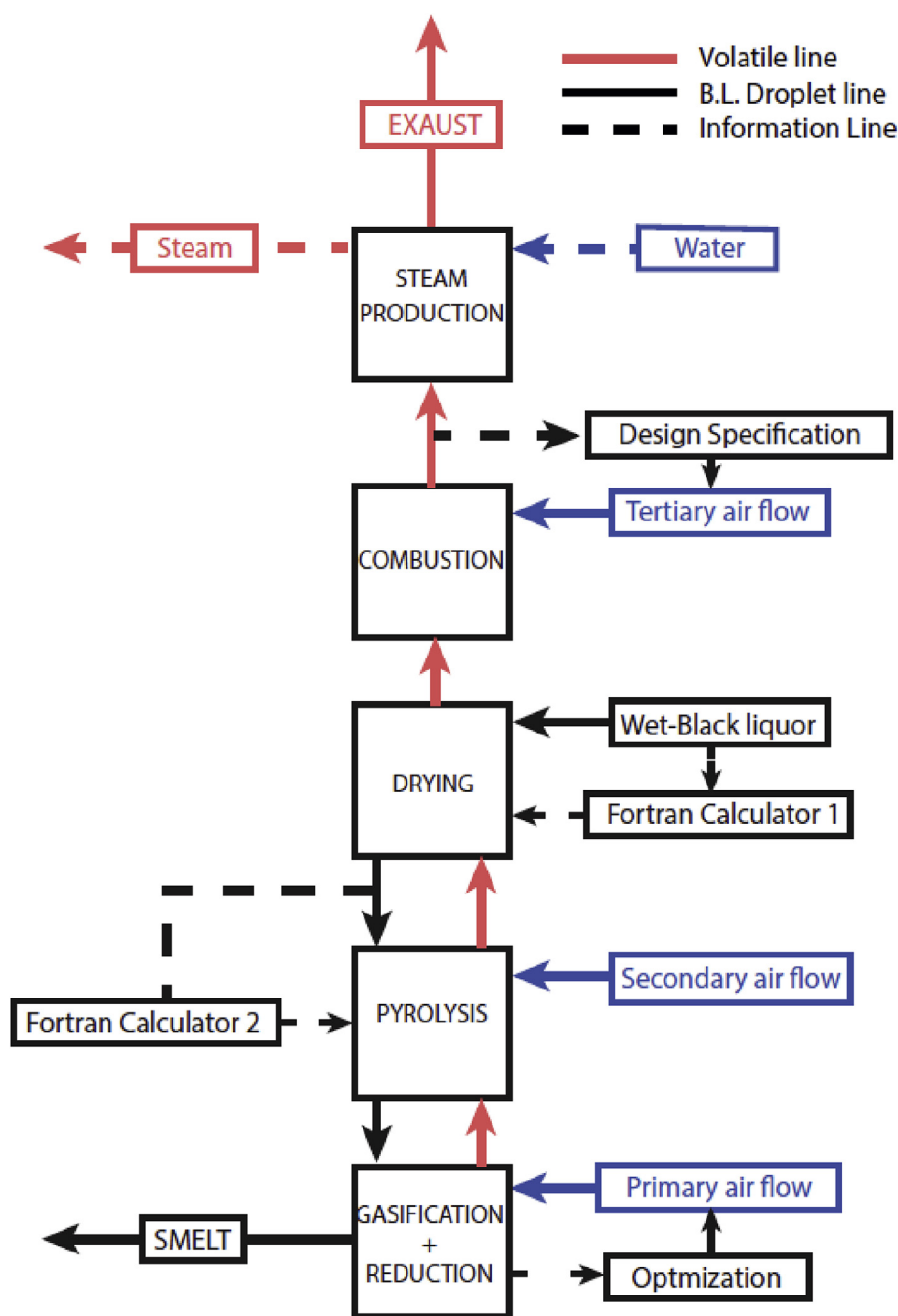
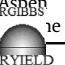

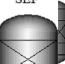







Fig. 3. Flowsheet of a recovery boiler in Aspen Plus®.

**Table 4**  
Aspen Plus® routines used in the model.

Aspen Plus® Icon	Description	Utilization
	<b>RGibbs</b> – It predicts reactions without the need for stoichiometry, kinetics, and yield. Minimizes Gibbs free energy to determine products.	Used to predict the volatiles' combustion and the reduction reactions in the char bed.
	<b>RYield</b> – Predicts reactions based on yield. It does not require stoichiometry and kinetics.	Used to perform black liquor decomposition in conventional components.
	<b>RStoic</b> – Reaction modeling performed using stoichiometry.	Used to model the drying process of solid black liquor particles.
	<b>Sep</b> – Combines material flowrates and divides them into two or more chains, according to the stream class.	Used to predict the solid–gas separation that occurs throughout the boiler.
	<b>HeatX</b> – Performs heat transfer between hot and cold process streams.	Used in the heat transfer zone and responsible for using flue gas energy to generate superheated steam.
	<b>SSplit</b> – Combines material streams and divides the resulting stream into two or more streams.	Used to realize the thermal equilibrium between black liquor particles and flue gas.
	<b>Split</b> – Splits process stream into two or more streams.	Used to split the combustion air and the flue gas along the furnace.
	<b>Mixer</b> – Mixes process streams.	Used to mix process streams.

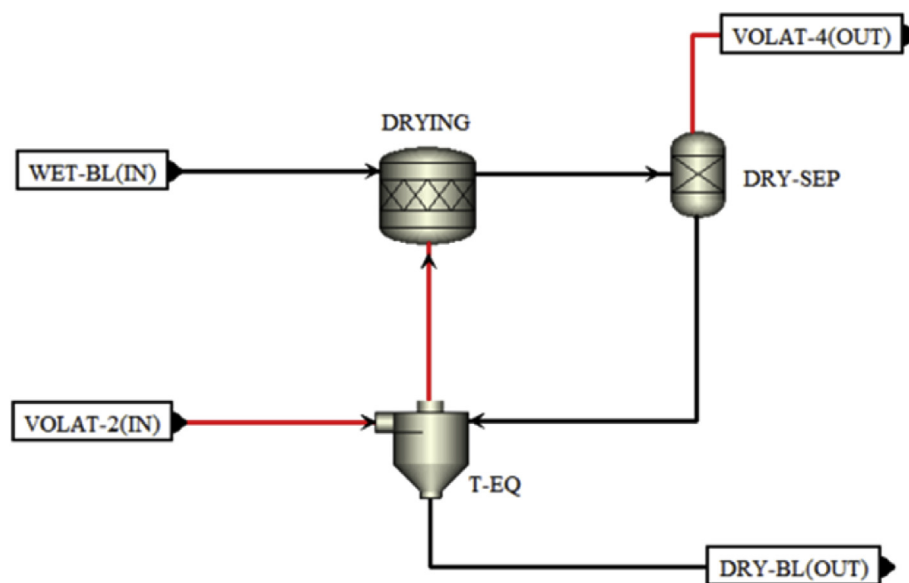


Fig. 4. Process flow diagram of drying section.

The evaporation of moisture is represented by



Because the black liquor is a nonconventional component, the simulator considers that its molar mass is equal to 1 g/mol. As the molar mass of water is 18.015 g/mol, the stoichiometry of the reaction above can be deduced, i.e., the reaction above indicates that 1 mol of wet black liquor reacts to form 0.055 mol of water.

Although black liquor drying was not considered a chemical reaction, the RStoic model (DRYING Block) was used to convert a portion of the wet black liquor to form water (Eq. (1) was used to simulate the extent to which drying occurred).

To calculate the drying rate, the Aspen Plus® Calculator was used, and Eq. (2) was implemented (Fortran Calculator 1 – a tool where equations can be implemented by using Fortran programming language). In this study, it was considered that after the drying process, the black liquor was completely dry, i.e., no moisture remained. Eq. (2) shows the result of combining water balance and global mass balance.

$$Conv = \frac{H2O^{in} - H2O^{out}}{100 - H2O^{out}}, \quad (2)$$

where.

$Conv$  is the drying efficiency;

$H2O^{in}$  is the percentage of water in wet black liquor;

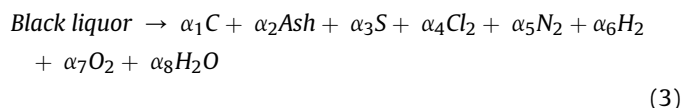
$H2O^{out}$  is the percentage of water in dry black liquor.

The T-EQ block (SSplit) was used to guarantee thermal equilibrium between the dry black liquor, which moved to the pyrolysis section, and the volatiles, which are from the bottom of the boiler. The DRY-SEP block (Sep model) was used to separate the products of the drying process, the water vapor, and the dry black liquor droplets.

#### 3.4.2. Pyrolysis section

The dry black liquor moved to the pyrolysis region (immediately below the drying stage), where the volatiles were released, as shown in Fig. 5.

To perform pyrolysis, the DECOMP (RYield model) and PYRO-REA (RGibbs model) blocks were required. DECOMP performed a hypothetical decomposition of the black liquor based on its ultimate analysis, as shown in Eq. (3), resulting in a homogeneous mixture of elemental substances  $\text{H}_2\text{O}$ , ash, C,  $\text{H}_2$ ,  $\text{N}_2$ ,  $\text{Cl}_2$ , S, and  $\text{O}_2$ .



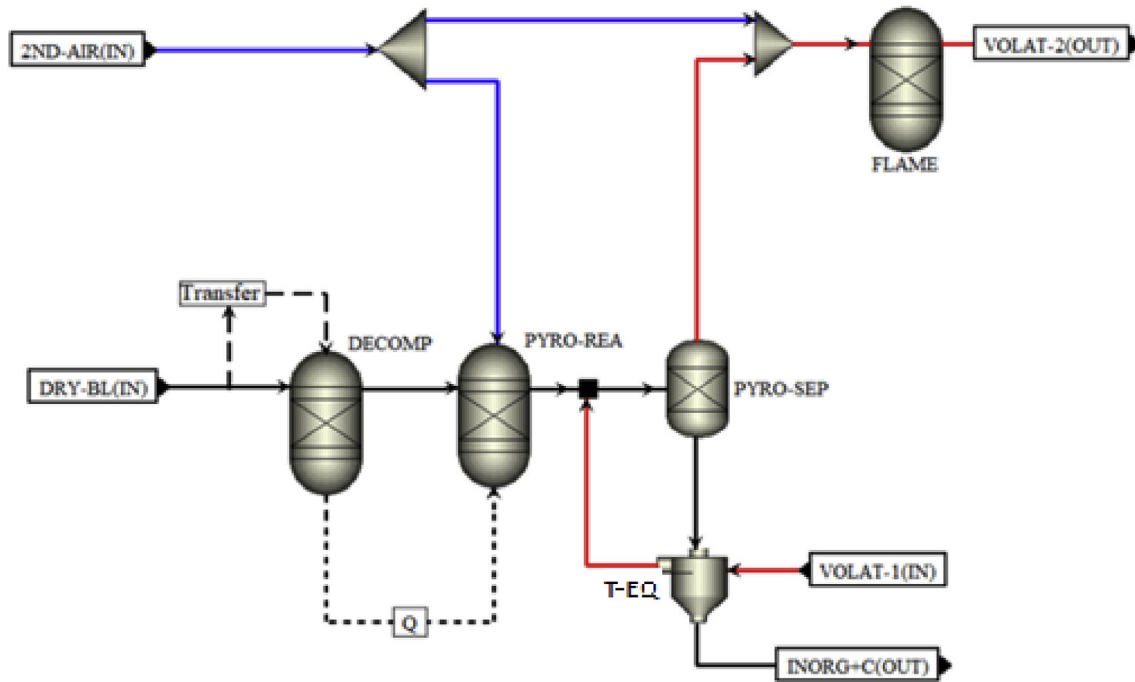


Fig. 5. Process flow diagram of pyrolysis section.

RYield (DECOMP) was used to model the black liquor decomposition based on the black liquor ultimate analysis. Fortran Calculator 2 was used to obtain the component yield, according to Eqs. (4) and (5). It is noteworthy that  $\text{Na}_2\text{CO}_3$ ,  $\text{Na}_2\text{SO}_4$  and Na were not decomposed, as those elements could not be inserted as an ultimate analysis into the software. These elements were therefore inserted as *CISOLID* in the black liquor feed. Hence, it was necessary to normalize the mass fractions of the other components present in Table 2 before inserting them into the simulator. Eq. (4) and Eq. (5) were multiplied by a normalization factor of 0.70, which refers to the difference between the total mass composition and the portion of the *CISOLID* components mentioned above. The sum of all components (Eq. (4) to Eq. (8)) present in the black liquor feed must be equal to 1.

$$\alpha_{1,\dots,7} = \frac{ULT_i}{100} * 0.70 \quad (4)$$

$$\alpha_8 = \frac{PROX_i}{100} * 0.70 \quad (5)$$

$$X_{\text{Na}_2\text{CO}_3} = 0.09 \quad (6)$$

$$X_{\text{Na}_2\text{SO}_4} = 0.06 \quad (7)$$

$$X_{\text{Na}} = 0.14 \quad (8)$$

where:

$\alpha_{1,\dots,8}$ : ash, carbon,  $\text{H}_2$ ,  $\text{N}_2$ , S,  $\text{O}_2$ , and  $\text{Cl}_2$ ;

ULT: ultimate analysis;

PROX: proximate analysis.

The block "Transfer" was used to copy the temperature of the DRY-BL stream, and the value was used as the reference temperature in block DECOMP. Hence, the reference temperature used to calculate the energy required to decompose the black liquor will be the temperature of the black liquor droplets.

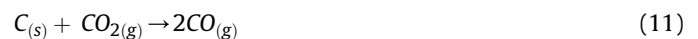
The constituent elements were sent to PYRO-REA, where pyrolysis occurred to release the volatiles ( $\text{CO}_2$ , CO,  $\text{H}_2$ ,  $\text{CH}_4$ ,  $\text{H}_2\text{O}$ ,  $\text{H}_2\text{S}$ , and mercaptans). As discussed earlier, the distribution of the chemical species was obtained by minimizing the Gibbs free energy. The volatiles combined with the gases from the lower region of the boiler and they moved together in an upward flow, whereas the inorganics moved to the bottom of the boiler (the SEP block performed this separation). The required heat for this section was provided by the Q energy stream, which represents the enthalpy change when the dry black liquor is decomposed into its constituent elements, resulting in a lower temperature of the volatiles at block PYRO-REA.

The pyrolysis section is an oxidizing zone, following which the released volatile matter combined with the secondary air and then combusted instantaneously, generating a combustion zone.

#### 3.4.3. Gasification and reduction section

Inorganics and the remaining fixed carbon flowed to the bottom of the boiler, where heterogeneous combustion and reduction reactions occurred, as shown in Fig. 6.

A portion of the carbon from the pyrolysis region was burned with the primary air in the GAS + RED block (RGibbs model). The main reactions that occurred in this section are listed below:



The gasification provided the required energy for the endothermic reactions in the reduction zone. The goal was to react the remaining carbon with  $\text{Na}_2\text{SO}_4$  to form  $\text{Na}_2\text{S}$ . However, other



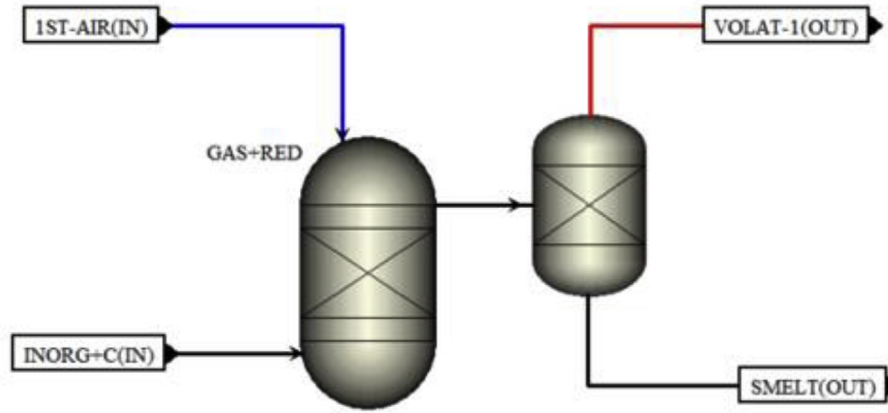
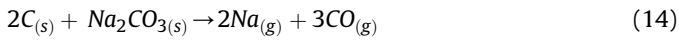
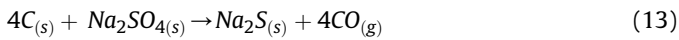


Fig. 6. Process flow diagram of gasification and reduction section.

reactions occurred but in a lesser extent, as follows:



The result of this stage was the formation of volatiles and smelt in a region known as the char bed. As described, this zone must have a reducing environment with no  $O_2$  to maximize the reduction efficiency. The smelt composition and reduction efficiency are measurable variables and can be estimated using the model developed. Mathematically, the reduction efficiency is expressed as shown in Eq. (16):

$$\text{Reduction Efficiency}(\%) = \frac{Na_2S \text{ (mol\%)}}{Na_2S \text{ (mol\%)} + Na_2SO_4 \text{ (mol\%)}} \quad (16)$$

The optimization tool (Optimization) was used to determine the primary air required to minimize the difference between the simulated and measured reduction efficiency (Eq. (17)). In this case, the primary air becomes the output of the model. This variable can be used to validate the model.

$$\text{Min } f = \left| \frac{Na_2S \text{ (mol\%)}}{Na_2S \text{ (mol\%)} + Na_2SO_4 \text{ (mol\%)}} \right| - RE \quad (17)$$

where  $ER$  is the measured reduction efficiency (industrial data).

For the optimization routines, the bound optimization by quadratic approximation method was used.

#### 3.4.4. Combustion section

The volatiles resulting from the lower region of the boiler flowed to the pyrolysis zone to be burned with the secondary air. Because the combustion can be incomplete, an additional combustion is required to burn the remaining carbon monoxide and sulfur gases (Fig. 7). In this case, a tertiary air input is used. Another task of the tertiary air is to form an air curtain to prevent the passage of particulates to the next region of the boiler; to represent this stage, the RGibbs model was used. Furthermore, the combustion zone supplies heat to the steam generation region.

In this zone, the design specification tool (Design Spec 1) was used to manipulate the tertiary air flow (Eq. (18)) to burn the remaining carbon monoxide and reach the target established in Eq. (19) (industrial data). Similar to the primary air, the tertiary air became an output variable.

$$40,000 \text{ Nm}^3 / \text{h} \leq \text{Tertiary Air Flow} \leq 50,000 \text{ Nm}^3 / \text{h} \quad (18)$$

$$\text{CO Mass Fraction} (X_{CO}) = 1,236 \text{ ppm} \quad (19)$$

#### 3.4.5. Steam generation

The upper furnace transforms liquid water into superheated, high-pressure steam using heat exchange between combustion gases and water-steam system. It is also known as the convective heat transfer zone. The steam generation process, represented in Fig. 8, shows liquid water represented by the dashed blue line, steam by the dashed red line, and flue gases by solid red lines. During their upward flow, the gases exchange heat with the walls of the lower furnace, where water pipes were located. This heat transfer is represented by the WALL block. The gases then enter the

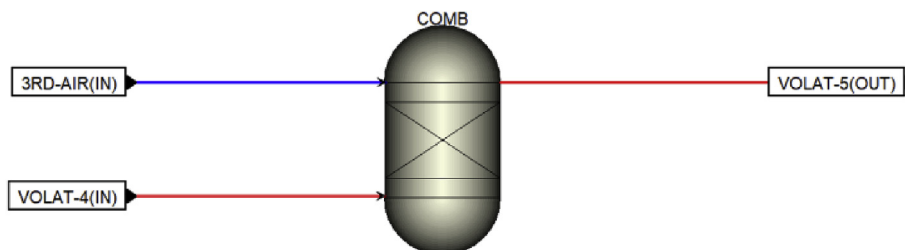


Fig. 7. Process flow diagram of combustion section.

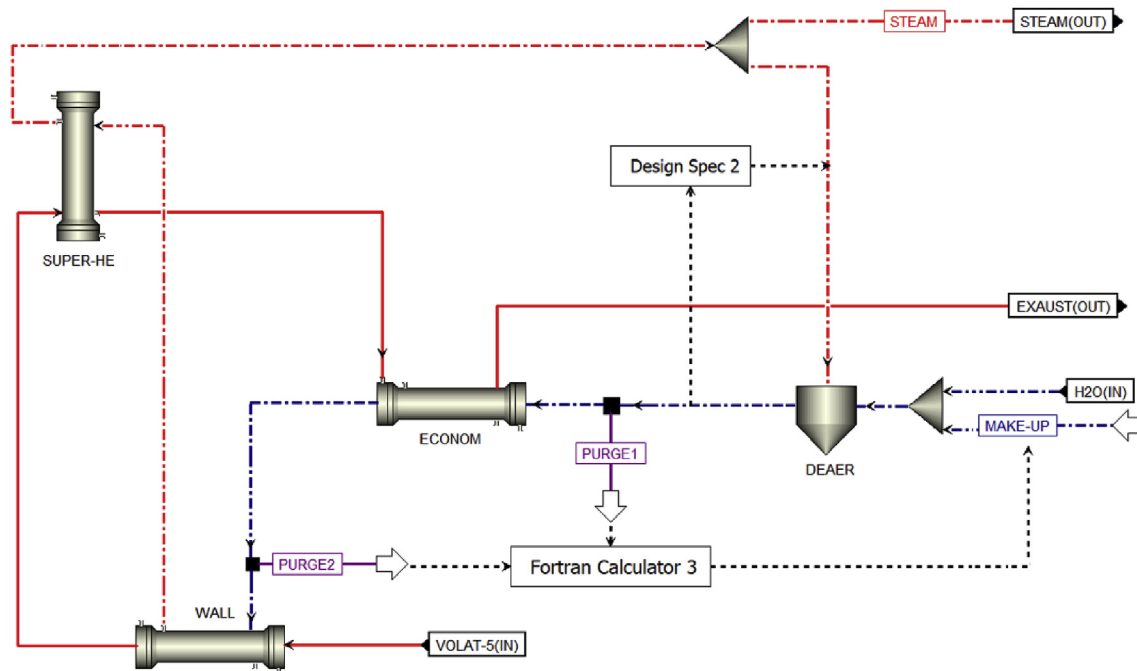


Fig. 8. Process flow diagram of higher furnace: steam generation.

$$0.05 \leq \text{split fraction} \leq 0.3 \quad (20)$$

$$T_{\text{FeedWater}} = 118^{\circ}\text{C} \quad (21)$$

higher furnace, where the superheater (SUPER-HE block), responsible for superheating the saturated steam that leaves the walls, is located. Finally, the gases enter the economizer (ECONOM block), where liquid water is preheated, and ultimately to the exhaust. In a simplified form, these steps can be represented by the set of heat exchangers (HeatX) shown in Fig. 8. The heat exchange areas were used to establish the specifications. Hence, the temperatures obtained for this region were the result of the model.

As shown in Fig. 8, part of the superheated steam produced was used to preheat the water in the deaerator (DEAEER block) before it was fed to the boiler. The steam flow required to reach the feedwater temperature was calculated using Design Spec 2 by manipulating the split fraction (Eq. (20)) of the block SPLT, which separates the steam to be used in the plant from the steam for preheating the feedwater (Eq. (21)).

The steam generation involves two material losses: the vent at the deaerator (PURGE1) and blowdown (PURGE2). Fortran Calculator 3 was implemented to calculate the water make-up (MAKE-UP stream) to compensate for the water losses of the system:

$$\text{Makeup} = \text{Purge1} + \text{Purge2} \quad (22)$$

## 4. Results and discussion

The model was tested with data from Brazil's largest pulp and paper industry. Because the data provided were only for average operating conditions, the results for other conditions could not be evaluated. To overcome this restriction and to guarantee the accuracy of the model, data from previous studies were tested as well (Silva et al., 2008).

### 4.1. Model validation

Because flow rate and temperature measurements could not be obtained from inside the boiler, those variables could not be validated individually in each hierarchy of the process. Hence, the parameters used to validate the model were the production and composition of the smelt as well as the reduction efficiency, air flow rates, and green steam generation.

Table 5 shows the validation of the model, in which the results obtained for the production and molar composition of the physically active layer of the char bed were compared with industrial data. The error in the reduction efficiency was small because the result of the objective function (Eq. (17)) was  $1.4 \times 10^{-7}$ .

The error was calculated according to the following definition of relative error:

$$\text{Error}(\%) = \frac{|X_{\text{simulation}} - X_{\text{measured}}|}{X_{\text{measured}}} \times 100 \quad (23)$$

The primary and tertiary air flows were calculated in the model such that they can be used as validation variables. The secondary air flow was used as an input to the model. The tertiary air flow rate

Table 5

Model validation with industrial data: Smelt variables and reduction efficiency.

	Measured	Simulation	Error (%)
Production (kg/s)	6.80	6.92	1.7
Na <sub>2</sub> CO <sub>3</sub> (mol %)	0.77	0.76	1.0
Na <sub>2</sub> S (mol %)	0.21	0.22	3.5
Na <sub>2</sub> SO <sub>4</sub> (mol %)	0.02	0.02	3.1
Reduction Efficiency (%)	91.34	91.34	0.0

was used to obtain the carbon monoxide mass fraction in the exhaust established in Eq. (19). Table 6 shows the results of the air flow rates.

Because the secondary air flow rate was fixed and the primary air flow rate was manipulated to achieve the desired reduction efficiency, these false air inlet flows, which were not measured at the plant, affected the calculated tertiary air flow, resulting in a slightly higher error, as shown in Table 6.

Because of the production and composition of the smelt and the reduction efficiency being validated with the plant data, it was possible to verify the steam production obtained in the higher furnace section: 175 t/h of green steam at 50 bar (420 °C). Table 7 shows the results of the steam production.

Data from Silva et al. (2008) were directly obtained from CENIBRA's data acquisition system and used to test the present model. Thus, these literature data values were used as measured values as referred to in Eq. (23). The goal of his study was to predict the steady-state behavior of smelt composition in a recovery boiler by Gibbs free energy minimization. Silva's study involved different operational conditions from those tested earlier; however, the equipment configuration was similar to that used in this study. It is noteworthy that the smelt composition results of Silva's were normalized to the species of  $\text{Na}_2\text{CO}_3$ ,  $\text{Na}_2\text{S}$ , and  $\text{Na}_2\text{SO}_4$ . Table 8 shows the results obtained for smelt composition and reduction efficiency.

Additionally, validation of the model in terms of atmospheric emissions using an environmental approach was achieved. The results of the exhaust gas composition are shown in Table 9.

The focus of Silva's study was the reactive zone; therefore, only primary and secondary air flows were provided. The present model used the secondary air flow as input, and the primary air flow was calculated using Eq. (17); Table 10 shows the results.

As shown, the errors of both models were small in both cases (industrial and literature data). The validation results show that the model can estimate all the variables considered the most important in recovery boilers simultaneously: air flow rate, smelt composition, exhaust gas composition, and green steam generation. By contrast, only one of these variables can be predicted at one time in previous studies.

#### 4.2. Sensitivity analysis of reduction efficiency

Reduction efficiency is one of the variables that indicate whether the boiler is operating appropriately, i.e., if it is recovering the inorganic compounds present in the white liquor. Hence, industrial plant managers seek operating conditions that can maximize this efficiency. The developed model allows one to evaluate the effect of air feed on reduction efficiency. The main steps in the black liquor combustion process are directly affected by the primary and secondary air. Therefore, a sensitivity analysis of these variables was performed, as shown in Fig. 9.

In Fig. 9, each curve is associated with a fixed secondary air flow. As the primary air flow changes, a new operating condition appears with the corresponding reduction efficiency. All the cases studied have the same air supply variation tendency. However, it was observed that the reduction efficiency was significantly affected by

**Table 7**

Model validation with industrial data: green steam production.

Variable	Measured	Simulation	Error (%)
Flow rate (t/h)	175	175	—
Temperature (°C)	420	429	2.14
Exhaustion temperature (°C)	190	196	3.06

**Table 8**

Model validation with literature data: smelt composition and reduction efficiency.

Variable	Silva (2008)	This work	Error (%)
$\text{Na}_2\text{CO}_3$ (mol %)	0.66	0.65	1.90
$\text{Na}_2\text{S}$ (mol %)	0.31	0.32	3.77
$\text{Na}_2\text{SO}_4$ (mol %)	0.03	0.03	3.00
Reduction Efficiency (%)	92.70%	92.15%	0.60

**Table 9**

Model validation with literature data: exhaust gas composition (molar fraction).

Variable	Silva (2008)	This work	Error (%)
$\text{O}_2$ (mol %)	0.000	0.000	0.00
$\text{N}_2$ (mol %)	0.629	0.601	3.97
$\text{H}_2$ (mol %)	0.050	0.053	6.00
$\text{H}_2\text{O}$ (mol %)	0.116	0.125	7.75
$\text{CO}$ (mol %)	0.087	0.092	4.60
$\text{CO}_2$ (mol %)	0.118	0.112	4.23
$\text{H}_2\text{S}$ (mol %)	0.000	Trace	0.00
$\text{SO}_2$ (mol %)	0.000	Trace	0.00
$\text{CH}_4\text{S}$ (mol %)	0.0001	Trace	0.00
$\text{CH}_4$ (mol %)	0.000	0.000	0.00

**Table 10**

Model validation with literature data: air flow rate.

Variable	Silva (2008)	This work	Error (%)
Primary Air (t/h)	162.02	154.16	4.85
Secondary Air (t/h)	164.65	164.65	—

the primary air flow rate in an inversely proportional manner. It is vital that the amount of primary air supplied is as such to ensure a reducing atmosphere because most of the  $\text{O}_2$  must be consumed by carbon; however, sufficient carbon must remain to react with  $\text{Na}_2\text{SO}_4$  to ensure a high reduction efficiency for  $\text{Na}_2\text{S}$  formation. The secondary air flow rate may affect the amount of carbon at the bottom of the boiler because of the possibility of carbon being converted to gaseous oxides before reaching the active layer of the char bed. However, the main function of the secondary air is to perform the combustion of released volatiles during the pyrolysis step, which does not affect the reduction efficiency, as shown in Fig. 9.

Furthermore, Fig. 9 shows that for a fixed primary air flow of 45,000  $\text{Nm}^3/\text{h}$ , all the cases presented herein this paper reached a reduction efficiency exceeding 92%, which is expected in industrial plant operations.

**Table 6**

Model validation with industrial data: air flows.

Variable	Temperature (°C)	Measured ( $\text{Nm}^3/\text{h}$ )	Simulation ( $\text{Nm}^3/\text{h}$ )	Error (%)
Primary Air	150	45,460	45,140	0.7
Secondary Air	157	88,960	88,960	—
Tertiary Air	38	44,163	47,220	6.9

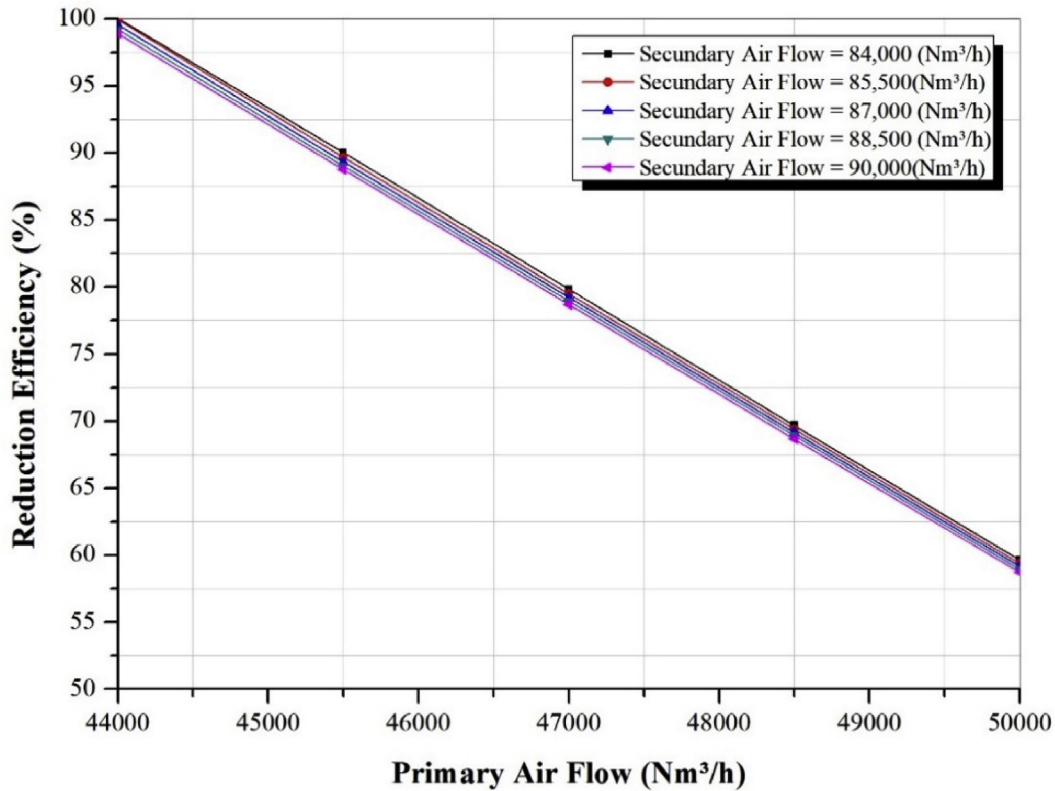


Fig. 9. Analysis of sensitivity to air flows: reduction efficiency performance.

#### 4.3. Sensitivity analysis in steam production

The present topic pertains to the possibility of increasing green steam production while maintaining the lower heating value of the black liquor. Hence, a sensitivity analysis was performed on the primary, secondary, and tertiary air flow rates and the water feed. Some constraints were imposed in the analysis, which limited the viable results of the model. The constraints were as follows:

- ✓ Constant feed, with dry solid content of 70%;
- ✓ Maximum CO emission of 1236 ppm;
- ✓ Reduction efficiency of at least 91.34%;
- ✓ Steam production at 420 °C.

The lower and upper limits of the uncertainty intervals of each manipulated variable were defined according to Eq. (24)–(27):

$$175 < f_{\text{steam}}(t/h) < 180 \quad (24)$$

$$40,000 < f_{\text{air}}^{\text{primary}} \left( \text{Nm}^3/h \right) < 50,000 \quad (25)$$

$$85,000 < f_{\text{air}}^{\text{secondary}} \left( \text{Nm}^3/h \right) < 95,000 \quad (26)$$

$$47,000 < f_{\text{air}}^{\text{tertiary}} \left( \text{Nm}^3/h \right) < 57,000 \quad (27)$$

Table 11 shows the results obtained from the sensitivity analysis; the entire matrix contained thousands of scenarios. Owing to the large number of manipulated variables, ten points were adopted for each interval presented above. Each case represented a recovery boiler operating condition. The number of columns in this

matrix of results depended on the amount of information required.

The carbon monoxide mass fraction measured in the exhaust gases indicated that fuel was still available inside the low furnace. Hence, the temperature of the high-pressure steam can be increased by increasing the air supply in the boiler, thereby increasing the energy supplied for steam generation.

Owing to the restrictions imposed, many cases were not considered. However, an increase in the temperature of the steam produced with a fixed feedwater flow rate of 175 t/h was observed. This result indicates that the water flow rate can be increased and hence the green steam production (by 1 t/h).

The developed model enables a user to achieve other operation conditions that satisfy the desired specifications without the need for new investments.

#### 4.4. Industrial and environmental implications

Other boilers used for steam production in pulp and paper plants use natural gas as the fuel. The increase in steam production in the recovery boiler implies less need for steam production in natural gas boilers, as well as a reduction in carbon monoxide emissions into the atmosphere. Black liquor is preferred for environmental and economic reasons. As a byproduct, it would cause an environmental issue unless used as fuel in chemical recovery boilers. Additionally, it reduces the consumption of the highly expensive natural gas in conventional boilers. In other words, the improvement in thermal efficiency of the recovery boiler reduces the overall fossil fuel consumption and utility costs. An estimation of the potential gain related to the increase in green steam generation is based on the following assumptions:

- ✓ Steam price produced from black liquor (BL): \$8/t;

**Table 11**

Matrix obtained by sensitivity analysis: reduction efficiency, steam generation, and atmospheric emission (mass fraction).

Case	$f_{\text{primary}}^{\text{air}}$ (Nm <sup>3</sup> /h)	$f_{\text{secondary}}^{\text{air}}$ (Nm <sup>3</sup> /h)	$f_{\text{tertiary}}^{\text{air}}$ (Nm <sup>3</sup> /h)	Feedwater (t/h)	Reduction Efficiency (%)	$T_{\text{vap}}$ (°C)	$X_{\text{O}_2}$	$X_{\text{N}_2}$	$X_{\text{H}_2}$ (ppm)	$X_{\text{H}_2\text{O}}$	$X_{\text{CO}}$ (ppm)	$X_{\text{CO}_2}$	$X_{\text{TRS}}$	$X_{\text{SO}_x}$ (ppm)	$X_{\text{NO}_x}$ (ppm)
Base Case	45,140	88,960	47,220	175.0	91.34	429	0.008	0.61	329	0.14	1236	0.22	Trace	18	88
1	44,440	90,555	52,230	175.0	95.76	432	0.015	0.62	174	0.14	642	0.23	Trace	6	72
2	44,440	90,555	52,230	175.5	95.76	427	0.015	0.62	174	0.14	642	0.23	Trace	6	72
3	45,000	91,666	53,333	176.0	92.03	428	0.016	0.62	145	0.14	530	0.23	Trace	4	68
2102	45,555	95,000	51,111	175.0	87.58	428	0.016	0.62	136	0.14	494	0.24	Trace	3	64
6600	50,000	95,000	57,000	175.0	58.13	438	0.028	0.63	10	0.14	334	0.24	Trace	Trace	22

**Table 12**

Steam generation savings.

Steam Production (t/year)	Saving(\$/year)
8448	160,512

**Table 13**

Thermal savings from reduction in natural gas.

Reduction in natural gas (Nm <sup>3</sup> /year)	Savings (MWh/year)
675,840	6,74

- ✓ Steam price produced from natural gas (NG): \$27/t;
- ✓ Operating time: 8448 h.

The price of steam was obtained directly from the industry with reference to the rates in 2018. Because the increase in green steam is the same as in the decrease in the conventional boiler, the economic gain can be calculated as follows:

$$\text{Saving} \left( \frac{\$}{\text{year}} \right) = \text{Extra Green Stream} * (\text{Price(NG)} - \text{Increasing(BL)}) \quad (28)$$

This study showed an increase of 1 t/h in green steam in the recovery boiler. Table 12 presents the result of this improvement.

Considering that the average lower calorific value of natural gas is 35,982.4 kJ/Nm<sup>3</sup>, savings can be achieved in terms of thermal energy according to the following equation:

$$\text{Saving} \left( \frac{\text{MWh}}{\text{year}} \right) = \text{Saving} \left( \frac{\text{Nm}^3}{\text{year}} \right) * \text{LHV} \left( \frac{\text{MWh}}{\text{Nm}^3} \right) \quad (29)$$

As an average of 80 Nm<sup>3</sup>/h of natural gas is required to produce 1 t/h of superheated steam, the reduction in the consumption of natural gas in conventional boilers can be calculated. Table 13 shows the savings in thermal energy and natural gas.

The recommendation was to verify the tradeoff between the gain with the increase in steam generation and the economic loss in the recovery of Na<sub>2</sub>S. All the prices were collected in 2018 from industry.

## 5. Concluding remarks

Unlike previous models, the developed model can predict the reduction efficiency and green steam generation in chemical recovery boilers simultaneously. The phenomenological model was validated with data from the largest pulp and paper mill in Latin America as well as with data from previous studies.

A reduction efficiency of 91.34% was yielded in a steam

production of 175 t/h at 420 °C. A sensitivity analysis of the primary, secondary, and tertiary air flow rates showed that green steam generation can be increased by 1 t/h under the conditions established.

The increase in green steam production affected the environment significantly as it reduced the amount of natural gas consumed in conventional boilers as well as reduced CO, SO<sub>x</sub>, and NO<sub>x</sub> emissions into the atmosphere. The new scenario led to a reduction of 57, 77, and 22% in the emission of CO, SO<sub>x</sub>, and NO<sub>x</sub>, respectively.

Improved technological development fuels the ongoing demand for using competitive and environment friendly processes. The model developed in this study, though in good agreement with industrial data, can be improved further. For example, the model is equilibrium-based and the impact of gas–solid hydrodynamics has not been considered. External Fortran routine-based improvements can be incorporated in future enhancements for increased accuracy and flexibility.

## CRedit authorship contribution statement

**Arthur Damasceno:** Formal analysis, Conceptualization, Data curation, Funding acquisition, Writing - original draft. **Lucas Carneiro:** Writing - review & editing. **Nayana Andrade:** Writing - review & editing. **Suênia Vasconcelos:** Writing - review & editing. **Romildo Brito:** Writing - review & editing. **Karoline Brito:** Writing - review & editing, Formal analysis, Conceptualization, Data curation, Writing - original draft.

## Declaration of competing interest

The authors declare that they have no known competing financial interests or personal relationships that could have appeared to influence the work reported in this paper.

## Acknowledgements

The authors thank the Coordenação de Aperfeiçoamento de Pessoal de Nível Superior (CAPES) for their financial support toward this study.

## References

- Aspentech, 2001. Aspen Physical Property System.
- Azevedo, A., Alexandre, J., Marvila, M., Xavier, G., Monteiro, S., Pedrotti, L., Rangel, Afonso, 2020. Technological and environmental comparative of the processing of primary sludge waste from paper industry for mortar. J. Clean. Prod. 249. <https://doi.org/10.1016/j.jclepro.2019.119336>.
- Bhardwaj, S., Bhardwaj, N., Negi, Y., 2018. Cleaner approach for improving the papermaking from agro and hardwood blended pulps using biopolymers. J. Clean. Prod. 213. <https://doi.org/10.1016/j.jclepro.2018.12.143>.
- Blasio, C., Gisi, S., Molino, A., Simonetti, M., Santarelli, M., Björklund-Sänkiahio, M., 2019. Concerning operational aspects in supercritical water gasification of kraft



- black liquor. *Renew. Energy* 130. <https://doi.org/10.1016/j.renene.2018.07.004>.
- Cardoso, M., Avelar Costa, G., Oliveira, E., Ravagnani, S., 2012. Simulation of eucalyptus kraft black liquor combustion in industrial recovery boilers. *Lat. Am. Appl. Res.* 42.
- Costa, A., Biscoia, E., Lima, E., 2004. Mathematical description of the kraft recovery boiler furnace. *Comput. Chem. Eng.* 14. [https://doi.org/10.1016/S1570-7946\(03\)80249-3](https://doi.org/10.1016/S1570-7946(03)80249-3).
- EIA, 2017. Electric power monthly with data for june 2017. <https://doi.org/10.1590/S0104-66322008000300017>.
- Ferreira, D., Cardoso, M., Park, S., 2010. Gas flow analysis in a Kraft recovery boiler. *Fuel Process. Technol.* 91. <https://doi.org/10.1016/j.fuproc.2010.02.015>.
- Gagliano, A., Nocera, F., Bruno, M., Cardillo, G., 2017. Development of an Equilibrium-Based Model of Gasification of Biomass by Aspen Plus, 111. *Energy Procedia*. <https://doi.org/10.1016/j.egypro.2017.03.264>.
- Gautam, R., Seider, W., 1979. Computation of phase and chemical equilibrium: Part III. Electrolytic solutions. *AIChE J.* 25. <https://doi.org/10.1002/aic.690250612>.
- Ghaffari, S., Romagnoli, J., 2003. Steady state and dynamic behaviour of Kraft recovery boiler. *Comput Aided Chem Eng* 14. [https://doi.org/10.1016/S1570-7946\(03\)80251-1](https://doi.org/10.1016/S1570-7946(03)80251-1).
- Grace, T., 1992. *Chemical Recovery in the Alkaline Pulping Processes*.
- Han, J., Liang, Y., Hu, J., Qin, L., Street, J., Lu, Y., 2017. Modeling downdraft biomass gasification process by restricting chemical reaction equilibrium with Aspen Plus. *Energy Convers. Manag.* 153. <https://doi.org/10.1016/j.enconman.2017.10.030>.
- Hana, U., 2013. Competitive advantage achievement through innovation and knowledge. *Journal of Competitiveness* 5. <https://doi.org/10.7441/joc.2013.01.06>.
- Hu, X., Jarnerud, T., Karasev, A., Jonsson, P., Wang, C., 2020. Utilization of fly ash and waste lime from pulp and paper mills in the Argon Oxygen Decarburization process. *J. Clean. Prod.* 261. <https://doi.org/10.1016/j.jclepro.2020.121182>.
- Jones, A., 1989. *A Model of Kraft Recovery Furnace*. The institute of Paper Chemistry. Doctor's Thesis.
- Leppänen, A., Tran, H., Taipale, R., Välimäki, E., Oksanen, A., 2014. Numerical modeling of fine particle and deposit formation in a recovery boiler. *Fuel*. <https://doi.org/10.1016/j.fuel.2014.03.046>.
- Lide, D., 2003. *CRC Handbook of Chemistry and Physics, 84th Edition, 2003-2004*. Handb Chem Phys.
- Maakala, V., Järvinen, M., Vuorinen, V., 2018. Computational fluid dynamics modeling and experimental validation of heat transfer and fluid flow in the recovery boiler superheater region. *Appl. Therm. Eng.* 139. <https://doi.org/10.1016/j.applthermaleng.2018.04.084>.
- Machová, V., Vochozka, M., 2019. Analysis of Business Companies Based on Artificial Neural Networks, 61. SHS Web Conf. <https://doi.org/10.1051/shsconf/20196101013>.
- Mardoyan, A., Braun, P., 2015. Analysis of Czech subsidies for solid biofuels. *Int. J. Green Energy* 12. <https://doi.org/10.1080/15435075.2013.841163>.
- Munoz, P., Letelier, V., Zamora, D., Morales, M., 2020. Feasibility of using paper pulp residues into fired clay bricks. *J. Clean. Prod.* 262. <https://doi.org/10.1016/j.jclepro.2020.121464>.
- Pérez, M., Vakkilainen, E., 2019. A comparison of turbulence models and two and three dimensional meshes for unsteady CFD ash deposition tools. <https://doi.org/10.1016/j.fuel.2018.10.066>.
- Pérez, M., Vakkilainen, E., Hyppänen, T., 2016a. Fouling growth modeling of kraft recovery boiler fume ash deposits with dynamic meshes and a mechanistic sticking approach. *Fuel*. <https://doi.org/10.1016/j.fuel.2016.08.045>.
- Pérez, M., Vakkilainen, E., Hyppänen, T., 2016b. Unsteady CFD analysis of kraft recovery boiler fly-ash trajectories, sticking efficiencies and deposition rates with a mechanistic particle rebound-stick model. <https://doi.org/10.1016/j.fuel.2016.05.004>.
- Qin, S., Chang, S., 2017. Modeling, thermodynamic and techno-economic analysis of coke production process with waste heat recovery. *Energy* 141. <https://doi.org/10.1016/j.energy.2017.09.105>.
- Sainlez, M., Heyen, G., 2011. Recurrent neural network prediction of steam production in a Kraft recovery boiler. <https://doi.org/10.1016/B978-0-444-54298-4.50135-5>.
- Shahbaz, M., Yusup, S., Inayat, A., Ammar, M., Patrick, D., Pratama, A., 2017. Syngas Production from Steam Gasification of Palm Kernel Shell with Subsequent CO<sub>2</sub> Capture Using CaO Sorbent: an Aspen Plus Modeling, 31. *Energy and Fuels*. <https://doi.org/10.1021/acs.energyfuels.7b02670>.
- Silva, W., Ribeiro, J., Costa, E., Costa, A., 2008. Reduction efficiency prediction of cenibra's recovery boiler by direct minimization of Gibbs free energy. *Braz. J. Chem. Eng.* 25. <https://doi.org/10.1590/S0104-66322008000300017>.
- Smook, G., 1989. *Handbook for Pulp and Paper Technologists*.
- Tomlinson, C., Richter, F., 1969. *The Alkali Recovery System (Chapter 10) in Pulp and paper manufacture. Vol. I. The Pulping of Wood*. McGraw-Hill.
- Ungerma, O., Dedkova, J., Gurinova, K., 2018. The impact of marketing innovation on the competitiveness of enterprises in the context of industry 4.0. *Journal of Competitiveness* 10. <https://doi.org/10.7441/joc.2018.02.09>.
- Vochozka, M., Maroušková, A., Váchal, J., Straková, J., 2016. Reengineering the paper mill waste management. *Clean Technol. Environ. Pol.* 18. <https://doi.org/10.1007/s10098-015-1012-z>.
- White, C., Seider, W., 1981. Computation of phase and chemical equilibrium, part IV: approach to chemical equilibrium. *AIChE J.* 27. <https://doi.org/10.1002/aic.690270316>.
- Yu, C., Dijkema, G., Jong, M., Shi, H., 2015. From an eco-industrial park towards an eco-city: a case study in Suzhou, China. *J. Clean. Prod.* 102. <https://doi.org/10.1016/j.jclepro.2015.04.021>.
- Yu, C., Shi, L., Wang, Y., Chang, Y., Cheng, B., 2016. The eco-efficiency of pulp and paper industry in China: an assessment based on slacks-based measure and Malmquist-Luenberger index. *J. Clean. Prod.* 127. <https://doi.org/10.1016/j.jclepro.2016.03.153>.
- Zhang, Y., Cao, S., Shao, S., Chen, Y., Liu, S., Zhang, S., 2011. Aspen Plus-based simulation of a cement calciner and optimization analysis of air pollutants emission. *Clean Technol Environ Policy* 2011 13. <https://doi.org/10.1007/s10098-010-0328-y>.